Chemical Science

EDGE ARTICLE

View Article Online
View Journal | View Issue

Check for updates

Cite this: *Chem. Sci.*, 2017, **8**, 6542

A general and facile chemical avenue for the controlled and extreme regulation of water wettability in air and oil wettability under water†

Dibyangana Parbat,‡ Sana Gaffar,‡ Adil Majeed Rather, Aditi Gupta and Uttam Manna *

The controlled modulation of both oil (under water) and water (in air) wettability is an emerging approach to develop several functional materials for various prospective applications including oil/water separation, anti-corrosive coatings, underwater robotics, protein crystallization, drug delivery, open microfluidics, water harvesting *etc.* Here, we report a 'reactive' and covalently cross-linked coating through a facile and robust Michael addition reaction, which is suitable for the controlled and extreme regulation of both water and oil wettability in air and under water respectively. Along with extremes (super-philicity and super-phobicity) of water (in air) and oil (under water) wettability, this single multilayer construction was also able to display special liquid wettability (*i.e.*; extremely liquid repellent—but with controlled adhesive properties) both in air and under water, after strategic post chemical modifications, again through 1,4-conjugate addition reaction. The super-wetting properties in the materials were able to withstand various physical and chemical insults including adhesive tape test, sand drop test, and exposure to extremes of pH, salt, and surfactant contaminated aqueous media. Moreover, this approach also allowed the decoration of various flexible and rigid substrates (*i.e.*; wood, Al-foil, synthetic fabric *etc.*) with various bio-inspired wettability properties including (1) non-adhesive superhydrophobicity (lotus leaf), (2) adhesive superhydrophobicity (rose petal), (3) underwater superoleophobicity (fish scale) *etc.* This single polymeric coating—which is capable of displaying several bio-inspired interfaces both in air and under water, even after harsh physical/chemical insults—would be useful in various prospective and relevant applications for practical scenarios.

Received 22nd May 2017
Accepted 6th July 2017

DOI: 10.1039/c7sc02296d

rsc.li/chemical-science

Open Access Article. Published on 10 Mawuwani 2017. Downloaded on 2025-12-08 16:58:14.
This article is licensed under a Creative Commons Attribution-NonCommercial 3.0 Unported Licence.

Introduction

Bio-inspired heterogeneous wettability of liquids (oil/water)[1–5] on solid surfaces is instrumental in developing various advanced materials that are useful in widespread applications such as oil/water separation, drug delivery, protein crystallization, underwater robotics, water harvesting, open microfluidics *etc.*[6–20] The Cassie–Baxter model explains this extreme repellency of different liquids (oil and water) on solid surfaces by hypothesizing the presence of another phase (either air or water) on the solid surface,[21,22] which is responsible for the heterogeneous wettability of the liquids (oil/water). As an example, the metastable trapped air in the lotus leaf makes the solid surface extremely water repellent, where the water droplets bead with an advancing water contact angle (WCA) above 150°, and the droplets readily roll off on tilting the surface below 10°. Later, this anti-fouling property was recognized as superhydrophobicity.[23,24] Several top down and bottom up approaches[25,26] have been introduced in the literature to fabricate artificial superhydrophobic surfaces by following a general principle, where (1) hydrophilic building blocks are exploited following various processes to adopt the essential hierarchical topography (appropriate combination of micro/nano features)—which is (2) again coated with inert and low surface energy chemicals (composed of either fluorinated molecules or those with a long hydrocarbon tail), generally through a chemical vapor deposition process. However, the lack of a strong interaction between the hydrophilic hierarchical structures and inert low surface energy coating makes the material inherently fragile, and so it is susceptible to the loss of the anti-wetting property on exposure to harsh physical (bending, twisting, scratching *etc.*) or chemical (extremes of pH, salt *etc.*)

Department of Chemistry, Indian Institute of Technology-Guwahati, Kamrup, Assam 781039, India. E-mail: umanna@iitg.ernet.in

† Electronic supplementary information (ESI) available: A detailed experimental section is included in the ESI section and Fig. S1–S7 show a comparison of the growth of NC and change in the dipping solution which is a BPEI/5Acl mixture, post chemical functionalization of multilayers that are developed in the presence and absence of salt, SEM images of multilayers of NC and polymer, bouncing and rolling of oil/water, effect of chemical modification on liquid wettability, characterization of special adhesive-anti-fouling liquid (oil/water) wettability, and effect of various abrasive tests on the synthesized material. See DOI: 10.1039/c7sc02296d

‡ These authors have equal contribution to the work.

This journal is © The Royal Society of Chemistry 2017

Open Access Article. Published on 10 Mawuwani 2017. Downloaded on 2025-12-08 16:58:14.
This article is licensed under a Creative Commons Attribution-NonCommercial 3.0 Unported Licence.

insults.[27–31] Recently, a few elegant approaches have been introduced to develop durable superhydrophobic materials, yet the synthesis of durable superhydrophobic surfaces still remains a challenging and interesting research topic for fundamental and applied contexts.[32–37]

In 2009, a seminal report by Jiang and coworkers revealed the existence of another anti-fouling property of fish scales—which display extreme oil-repellency under water with an advancing oil contact angle (OCA) above 150° and a contact angle hysteresis below 10°.[3] Early demonstrations related to this anti-oil-fouling property revealed its prospective potential in the separation of oil/water emulsions, underwater robotics, anti-biofouling coatings, and in developing smart microfluidic devices *etc.*[7,9–11,14,18] Generally, metal oxides,[38–41] polymeric gels[3,14,18,42–45] and electrostatic multilayers[46,47] have been explored in developing appropriate topography and surface chemistry—which confer the desired heterogeneous oil-wettability under water through the impregnation and confinement of a water layer within the hierarchical topography of the coatings. These polymer gel, electrostatic multilayer and metal oxide approaches are useful for understanding the fundamentals related to this anti-oil-fouling property, but most often, these synthesized materials are liable to lose the embedded artificial anti-fouling property on exposing the materials to either harsh physical insults and/or complex chemical environments as (1) polymeric hydrogels are highly susceptible to easy deformation under regular physical/chemical manipulations and (2) metal oxide and electrostatic multilayers are known to corrode away under harsh chemical treatments.[48]

Nevertheless, these two completely distinct anti-fouling properties are undifferentiated in terms of the mode of wettability—a common heterogeneous (Cassie–Baxter state) liquid wettability is encountered in the respective materials, however, the entrapped third media are unambiguously different: (1) air for superhydrophobicity and (2) water for superoleophobicity under water.[2,3,21,22] As a consequence, the general requirements to stabilize the respective trapped media (air/water) in the respective materials are significantly different: (a) a hierarchical topography with a low surface energy is the basis to achieve metastable trapped air for superhydrophobicity,[1,2,23] whereas (b) superhydrophilic materials in air with appropriate micro/nano features are efficient for displaying extreme oil repellency underwater.[3–5] Here, in this article, we have introduced a single material that displays multiple durable super/special liquid wettability properties including superhydrophobicity in air and both superoleophobicity and superoleophilicity underwater through facile and precise control over the fraction of the solid contact area with beaded liquid phases both in air and under oil.

In our current design, a facile and robust 1,4-conjugate addition reaction between acrylate and amine groups is strategically exploited in the rapid construction of chemically 'reactive' thick coatings with the desired topography and chemical functionalities—which are essential parameters for adopting the desired special/super-liquid wettability in the synthesized material. First, amine 'reactive' nano-complexes (NCs) were synthesized from a BPEI/5Acl mixture, and constituted a multilayer coating by following a salt-assisted covalent and rapid layer-by-layer (LbL) deposition of the NCs in combination with the BPEI polymer. Then, the essential surface chemistry was adopted in the coating by strategic post chemical modification of the residual acrylate moieties in the multilayers of the NCs. Furthermore, the synthesized multilayers (9 bilayers of NC/BPEI) were explored for the gradual and extreme tailoring of both water wettability in air and oil wettability under water by controlling the fraction of the solid contact area with the respective beaded liquid phases through a facile change in both the chemical functionality and the topography of the material. Moreover, the materials displayed impeccable physical and chemical durability, and were able to withstand various kinds of insults without compromising the super-wetting properties of the materials. Furthermore, the current approach allows the decoration of various rigid/flexible substrates including wood, fabric, Al-foil *etc.* with desired super-anti-wetting properties. An example of such a single material—which is capable of coating various objects with desired physically/chemically durable super/special-liquid (water and oil) wettability properties both in air and under water—is unprecedented in the literature.

Results & discussion

Fabrication of multilayers of the nano-complexes and post chemical modification

In the past, the 1,4-conjugate addition reaction was strategically exploited in both the chemical modification (dendritic amplification of functional groups or selective modification of polymeric microstructures)[49,50] and the development of complex nanostructures (multilayer coatings and porous and moldable gels).[51,52] In relevance to our current design, in 2012, Lynn and Bechler explored this 1,4-conjugate addition reaction in the fabrication of a reactive and covalent multilayer, which was constructed by a mutual reaction between a polymer (branched polyethyleneimine, BPEI) and small molecule (dipentaerythritol penta-acrylate, 5Acl), and after 80 consecutive BPEI/5Acl layer depositions and appropriate post chemical modification, the material became only hydrophobic with a water contact angle ~138°.[52] Recently, we have reported the synthesis of a 'reactive' and moldable porous polymer gel by exploiting the facile Michael addition reaction[49–52] between the acrylate and amine groups of BPEI and 5Acl respectively, to develop a self-standing and three dimensional superhydrophobic shapeable monolith, where the polymeric gel material was formed *via* formation of the nano-complex (NC), and the formation of the gel was expedited in the presence of salt (NaCl).[53] In this current study, a stable nano-complex (NC) solution was first prepared by mixing BPEI/5Acl in methanol (Scheme 1B) both in the presence and absence of salt (0.5 mg ml^{-1}), which was later strategically embedded in the multilayer construction (Scheme 1D) in combination with the amine containing branched polymer (BPEI) by adopting a covalent LbL deposition process (Scheme 1C) through the 1,4-conjugate addition reaction (Scheme 1A) between the residual acrylate groups (in the NCs) and amine groups (in the BPEI polymer). During the study of the LbL

Open Access Article. Published on 10 Mawuwani 2017. Downloaded on 2025-12-08 16:58:14.
This article is licensed under a Creative Commons Attribution-NonCommercial 3.0 Unported Licence.

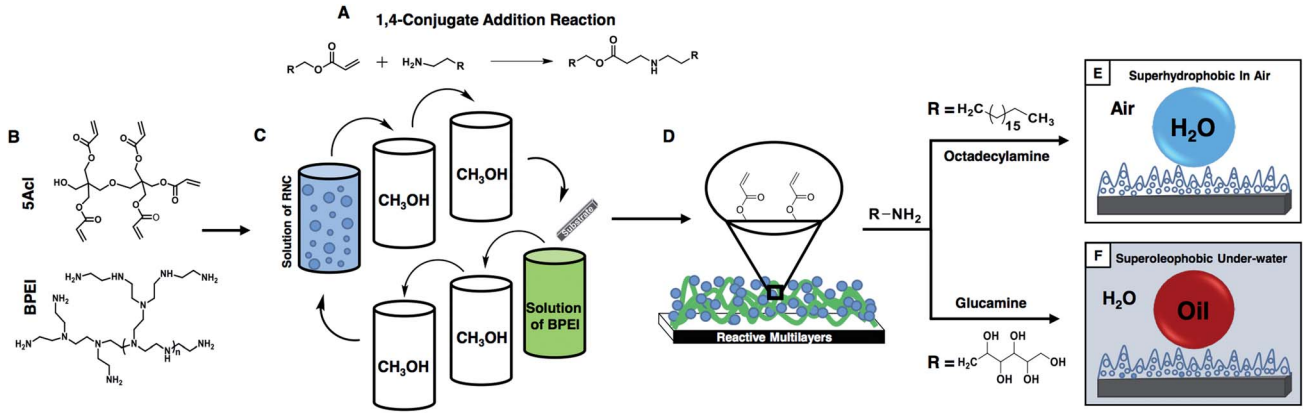

Scheme 1 (A) Schematic representation of the 1,4-conjugate addition reaction (Michael addition) between primary amine and acrylate moieties. (B) Structural formula of dipentaerythritol penta-acrylate (5Acl, top panel) and branched polyethyleneimine (BPEI, bottom panel). (C) Illustrating the formation of the 'reactive' nano-complexes (NCs) on mixing of BPEI and 5Acl in methanol, and their multilayer construction through the covalent layer-by-layer (LbL) deposition process in combination with the solution of BPEI. (D) Schematic representation of the multilayers of the NCs with residual acrylate groups. (E and F) Strategic post-chemical modifications of the multilayers of the NCs with appropriate small molecules (octadecylamine and glucamine) would provide extremes of liquid wettability both in air (superhydrophobicity, (E)) and under water (superoleophobicity, (F)).

deposition process, with an increasing number of LbL deposition cycles, an expedited growth in the size of the NCs was observed with the dipping solution of a BPEI/5Acl mixture which was doped with NaCl salt (0.5 mg ml^{-1}), as confirmed by a DLS study as shown in Fig. 1A. Later, the multilayer growth of the NCs (Scheme 1D) that were prepared both in the presence and absence of salt was monitored by measuring the thickness of the multilayers at regular intervals as shown in Fig. 1B. The growth of the multilayer of the NCs in the presence of salt was noticed to be exponential and yielded a thick (3.15 μm) multilayer coating after 9 bilayer (a pair of NC and BPEI layers are together designated as a single bilayer) depositions. However, the growth of the multilayers of the NCs that were prepared in the absence of salt was noticed to be sluggish and the thickness of the coating (9 bilayers of NC/BPEI) was measured to be only 830 nm. In comparison, the multilayers of the polymer that were directly constructed from BPEI and 5Acl solutions provided a coating with 700 nm thickness after 80 BPEI/5Acl layer depositions.[50] Thus, the strategic and rapid incorporation of the same components (BPEI and 5Acl) in the form of NCs in the covalent multilayers through the 1,4-conjugate addition[47–50] reaction allowed for high throughput synthesis of a thick and reactive polymeric coating.

Next, the topography of the coatings was examined with field emission scanning electron microscope (FESEM) imaging. At low magnification, the multilayers of the NCs that were fabricated in the presence of salt were found to have a prominent and random microstructure all around the coatings as shown in Fig. 1C and D, whereas, in the absence of salt, such dominated microstructures were not observed in the multilayers of the NCs, and rather, comparatively premature and smaller micro-domains appeared as evident from the images in Fig. 1F and G. These micro-domains in both of these multilayer coatings (that are prepared in the presence and absence of salt) are developed due to random arrangements of granular NC structures as evident from the FESEM images at higher magnification in Fig. 1E and H. As expected, the size of the granules are comparatively smaller in the multilayers of the NCs that are prepared in the absence of salt as shown in Fig. 1H, which is consistent with the DLS study in Fig. 1A where the growth of the NCs was observed to be rapid in the presence of salt, however the exact role of salt behind this expedited growth of NCs is not understood yet. This accelerated growth of the NCs and the difference in the size of the granular structures would have eventually influenced the growth of the micro-domains in the respective multilayers.

These multilayers of the NCs were further characterized by Fourier transform infrared (FTIR) spectroscopy, to investigate the available chemical functionalities in the multilayer construction. A characteristic IR peak (black curve in Fig. 1I) at 1413 cm^{-1} for the symmetric deformation of the C–H bond for the β carbon of the vinyl group was noticed in the multilayer of the NCs that was synthesized through consecutive LbL deposition of BPEI and NCs in the presence of salt. This IR signature confirmed the presence of residual acrylate groups in the multilayer of the NCs, and another IR peak at 1736 cm^{-1} revealed the presence of an ester carbonyl stretching in the multilayer construction.[49,50] Based on the past reports on the Michael addition reaction,[47–50] this carbonyl stretching most likely appeared due to β-amino ester-type cross-links in the multilayers through the repetitive 1,4-conjugate addition reaction between the amine and acrylate from BPEI and 5Acl respectively. Furthermore, the residual acrylate groups in the multilayers are suitable for post reaction with primary amine containing small molecules (glucamine and octadecylamine) through a 1,4-conjugate addition reaction, irrespective of their chemical functionalities (hydrophilic or hydrophobic). The successful post chemical modifications of the multilayers of the

This journal is © The Royal Society of Chemistry 2017

Open Access Article. Published on 10 Mawuwani 2017. Downloaded on 2025-12-08 16:58:14.
This article is licensed under a Creative Commons Attribution-NonCommercial 3.0 Unported Licence.

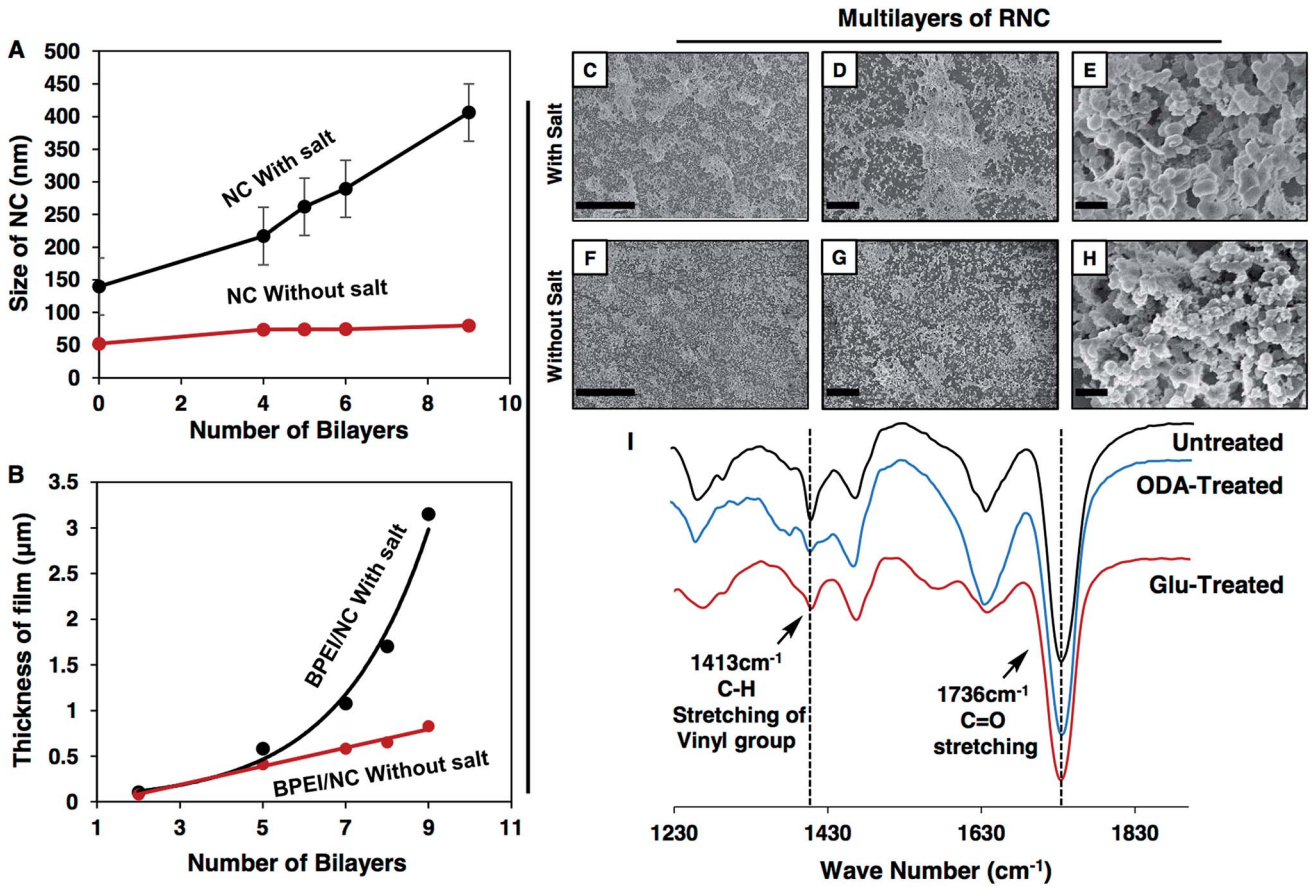

Fig. 1 (A) Illustrating the growth (size) of the nano-complexes (NCs) in the presence (black line, 0.5 mg ml^{-1}) and absence (red line) of NaCl salt in the LbL dipping solution of a BPEI/NC mixture during the construction of the multilayers. (B) A comparison of the growth (thickness) of the multilayers of the NCs with LbL deposition cycles both in the presence (black line) and absence (red line) of salt in the NC solution (one of the dipping solutions in the LbL deposition process). (C–H) Field emission scanning electron microscope (FESEM) images of the multilayers (9 bilayers) of the NCs in low ((C and F); scale bar = 20 μm), medium ((D and G); scale bar = 15 μm) and high ((E and H); scale bar = 500 nm) magnifications, which were constructed in the presence (C–E) and absence (F–H) of salt in BPEI/5AcI mixtures. (I) Fourier transform infrared (FTIR) spectra accounting for the chemical functionality in the multilayers of the NCs (that were constructed in the presence of salt) before (black line) and after post chemical modifications of the multilayers with strategically selected hydrophilic (glucamine, red line) and hydrophobic (octadecylamine, blue line) small molecules.

NCs with primary amine containing small molecules were analyzed by further FTIR study, where the characteristic peak at 1413 cm^{-1} for the residual acrylate groups was noticed to deplete significantly after post chemical modification as shown in Fig. 1I (the red and blue curves are for glucamine and ODA treatments, respectively), and all spectra are normalized with respect to the ester carbonyl functionality (at 1736 cm^{-1}) which is likely to remain unperturbed during the post chemical modification process. A very similar result was noticed with the multilayers of the NCs that are prepared in the absence of salt (see the ESI for more details, Fig. S2†).

Characterization of extreme liquid wettability in the multilayers of the NCs

The synthesized multilayers (9 bilayers) of the NCs, which are prepared in the presence and absence of NaCl salt, are noticed to be moderately hydrophobic in air with a CA of ~92° and 86° (Fig. 2A and D) respectively. However, after post chemical modification with ODA molecules (having a long hydrocarbon tail), the multilayer of the NCs which was constructed in the presence of salt became superhydrophobic with an advancing WCA of ~167° (Fig. 2B) and with a roll-off angle of 3° (Fig. 2K–N and S4G–J†). Moreover, a jet of water was noticed to immediately bounce away from the superhydrophobic surface as shown in Fig. 2O. In contrast, the hydrophobicity of the multilayer of the NCs that was prepared in the absence of salt was improved slightly and the water droplet had a WCA of ~104° after post chemical modification with the same ODA molecules as shown in Fig. 2E. Furthermore, with a gradual increase in the LbL deposition cycles from 2 to 9 bilayers, the change in water wettability in the post-modified (ODA) multilayers of the NCs (both in the presence and absence of salt) and BPEI polymer was examined in detail. The water repellency of the post modified (ODA treated) multilayer of the NCs was gradually increased with the number of LbL deposition cycles, the WCA was increased from 88° (2 bilayers) to 112° (7 bilayers), and

Open Access Article. Published on 10 Mawuwani 2017. Downloaded on 2025-12-08 16:58:14.
This article is licensed under a Creative Commons Attribution-NonCommercial 3.0 Unported Licence.

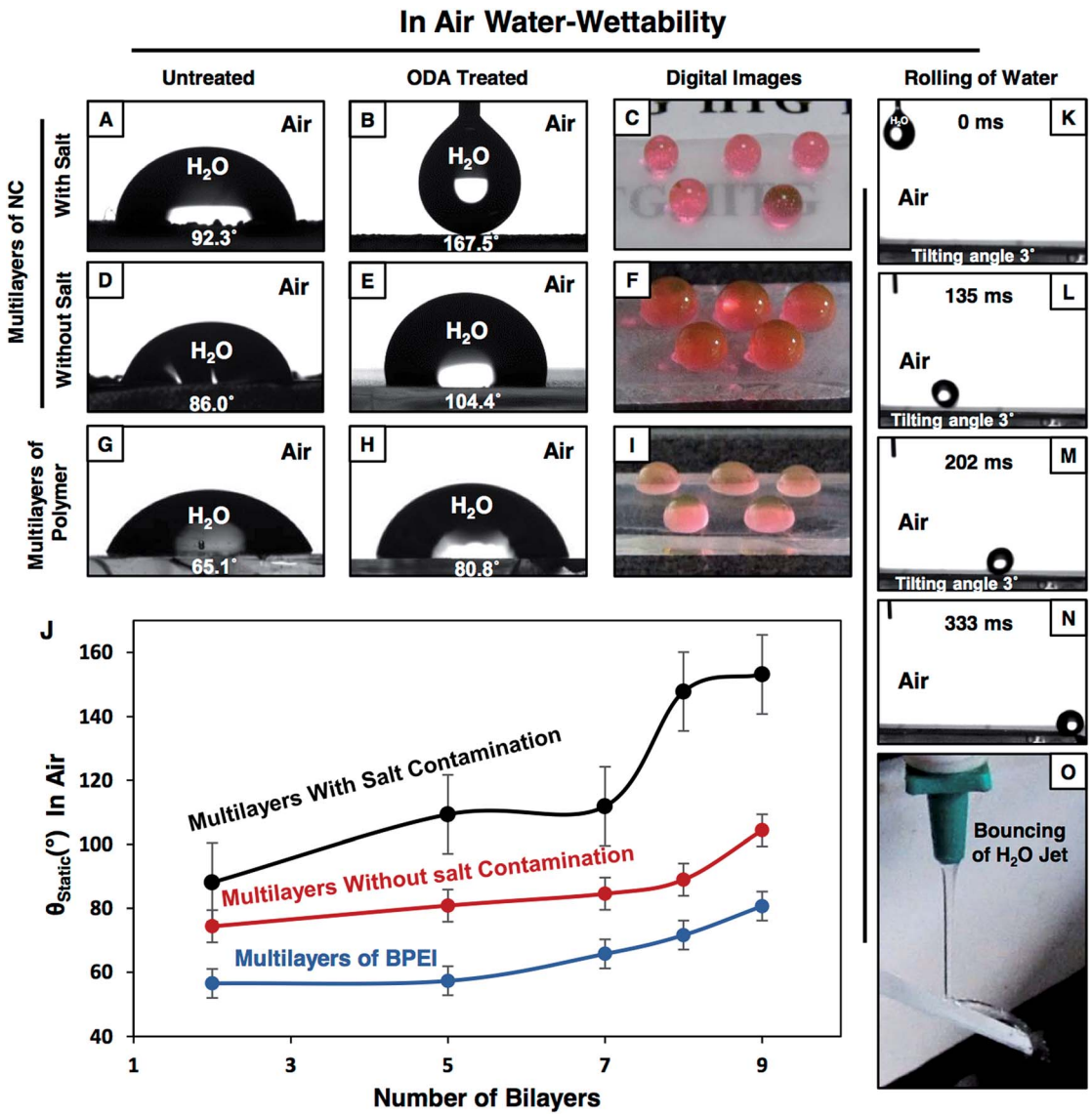

Fig. 2 (A–I) Contact angle measurements (A and B, D and E, and G and H) and digital images (C, F and I) of beaded water droplets (the red color aids visual inspection) on both the multilayers of the NCs (that were constructed in the presence (A–C) and absence (D–F) of salt) and BPEI polymer ((G–I); which was built in the presence of salt) before (A, D and G) and after (B and C, E and F, H and I) post chemical modification with ODA molecules. (J) A plot showing the change in the static water contact angle (WCA) of the beaded water droplets (4.5 μL) on ODA-treated multilayers of the NCs (built in the presence (black line) and absence (red line) of NaCl salt) and BPEI (in the presence of salt, blue line) in air with an increase in the number of bilayer deposition cycles. (K–N) Contact angle images showing the rolling of a water droplet (5 μL) on an ODA-treated multilayer of the NCs (which was synthesized in the presence of salt) that was tilted at 3° in air. (O) Digital image of a bounced water jet on the superhydrophobic surface.

suddenly, after 8 bilayer depositions, the hydrophobicity of the multilayer of the NCs was significantly improved with a static water contact angle (θ_{stat}) of ~148°, and the multilayer of the NCs was embedded with superhydrophobicity (θ_{stat} ~153°) after 9 bilayer depositions (black curve in Fig. 2J). However, the change in the WCA of the post modified multilayers of the NCs that were prepared in the absence of salt was noticed to be completely different, and the WCA was measured to be 104° even after 9 bilayer depositions (red curve in Fig. 2J). In another control study, the multilayer (9 bilayers) of BPEI polymer that was prepared in the presence of salt was found to be moderately hydrophobic with a θ_{stat} ~81° after post chemical modification with ODA molecules as shown in Fig. 2H.

On the other hand, the strategic post modification of the same multilayer (9 bilayers) of the NCs (that was fabricated in the presence of salt, and having an inherent static oil contact angle (OCA) ~31°, Fig. 3A) with hydrophilic small molecules (*i.e.*; glucamine) yielded a completely different anti-fouling property, which is recognized as underwater super-oleophobicity, where the oil droplet beaded with an advancing oil contact angle of ~169° underwater as shown in Fig. 3B, and the oil droplet rolled off on tilting the surface at 4°

 This journal is © The Royal Society of Chemistry 2017

Open Access Article. Published on 10 Mawuwani 2017. Downloaded on 2025-12-08 16:58:14.
This article is licensed under a Creative Commons Attribution-NonCommercial 3.0 Unported Licence.

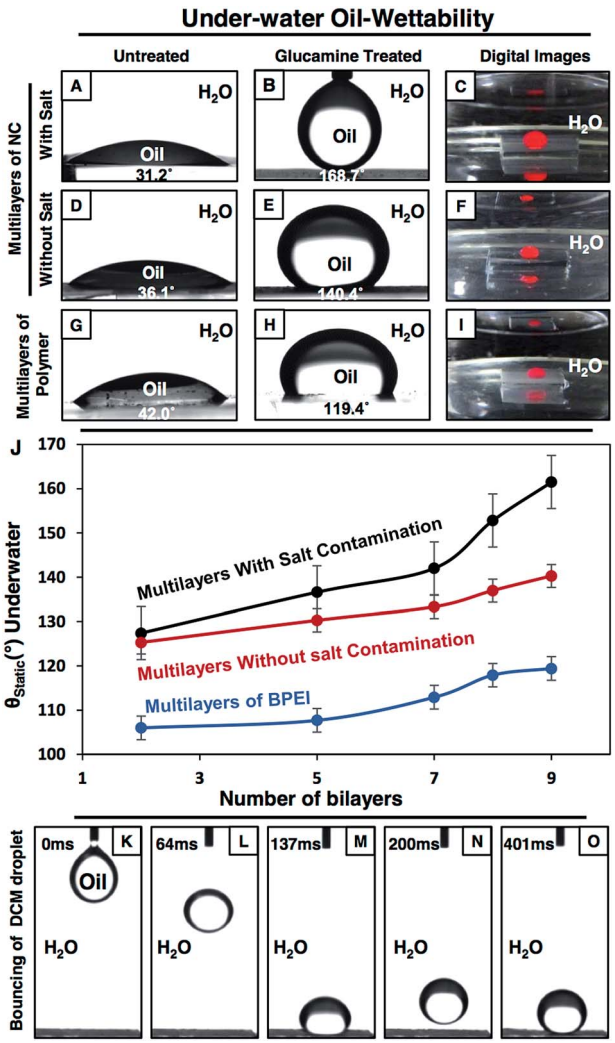

Fig. 3 (A–I) Contact angle images (A and B, D and E, and G and H) and digital images (C, F and I) show the underwater oil (the red color aids visual inspections) wettability on the multilayers (which were prepared in the absence (D–F) and presence (A–C and G–I) of NaCl salt) of both the NC/BPEI and BPEI/5Acl before (A, D and G) and after (B and C, E and F, and H and I) post chemical modification with glucamine molecules. (J) The change in static oil contact angle (OCA) on the glucamine treated multilayers of the NCs (black and red curves represent the multilayers which were prepared in the presence and absence of salt respectively) and polymer (BPEI, blue curve) with an increase in the number of deposition cycles is shown in the plot. (K–O) The bouncing of the oil droplet (DCM, 11 μL) on the glucamine treated multilayer (9 bilayers, and which was built in the presence of salt) of the NCs under water.

(Fig. S4K–O†). Moreover, an 11 μL DCM (model oil) droplet was observed to bounce on the surface as shown in Fig. 3K–O. In comparison, the multilayer (9 bilayers) of the NCs (having an inherent static OCA ~36° (Fig. 3D)) which was built in the absence of salt was observed to not display extreme oil-repellency under water even after post chemical modification with the same glucamine molecules (Fig. 3E). The oil droplet was beaded on the modified multilayer with a static OCA ~140° (Fig. 3E). Furthermore, the effect of the gradual increase in the number of bilayers on the oil-wettability from 2 to 9 bilayers was examined in the post modified (glucamine) multilayers of both NCs (that are fabricated in the presence/absence of salt) and polymer (BPEI) (Fig. 3J). The change in oil-wettability was observed to be more sluggish for the post modified (glucamine) multilayers of the polymer (compared to BPEI/5Acl)—the oil wettability was increased by only ~13° (Fig. 3J, blue curve) on increasing the bilayer deposition from 2 bilayers (θ_{stat} ~106°) to 9 bilayers (θ_{stat} ~119°; Fig. 3H and I), and the static oil contact angle was similarly increased (by ~15°) from ~125° (2 bilayers) to ~140° (9 bilayers) in the post modified multilayers of the NCs that were prepared in the absence of salt. However, the change in oil-wettability was noticed to be completely different in the modified multilayers of the NCs that were constructed in the presence of salt, and the static oil contact angle was increased significantly from ~125° (2 bilayers) to ~162° (9 bilayers) as shown in Fig. 3J (black curve). These significant changes in the pattern of liquid (water/oil) wettability in air and under water most likely arise from the difference in topography of the multilayers of the NCs that were fabricated in the presence and absence of NaCl salt. The change in micro-domains in the multilayers was already discussed in the previous section and the morphology of the multilayers of BPEI under FESEM was observed to be mostly featureless as shown in Fig. S3E and F.†

Controlled and extreme tailoring of liquid wettability

In the recent past, a few approaches have been introduced in the literature to control the liquid wettability through a change in topography[58–62] and chemistry[54–57] of the coatings. However, in most of the designs, either the topography was tailored by adopting a complex fabrication process[59–62] or different chemical functionality was introduced through delicate chemistry[55–57] (*i.e.*; metal–sulfur bond and metal–ion interaction). Here, (1) the reactive and covalent LbL deposition process inherently provides a simple avenue to control the topography of the multilayers, and (2) the amine reactive residual acrylate groups in the multilayers of the NCs further allows the modification of the polymeric coatings with a wide range of chemical functionalities through the facile 1,4-conjugate addition reaction. The multilayers of the NCs (from now, multilayers of the NCs will refer to the coatings which were built in the presence of salt) which initially had a WCA ~92° and an OCA ~31° displayed superhydrophilicity in air with a WCA of 0° and superoleophobicity under water with an OCA ~162° after post chemical modification with glucamine molecules (hydrophilic small molecules). However, on post modification of the same multilayers of the NCs with strategically selected primary amine containing small molecules—where the hydrocarbon tail length of the reacted small molecules was judiciously and progressively increased from $-C_3H_7$ (propylamine) to $-C_{18}H_{37}$ (octadecylamine)—the WCA (in air) of the beaded water droplet on the multilayers of the NCs was gradually increased from ~75° (propylamine) to 153° (octadecylamine) (Fig. 4A red curve), whereas the OCA of the beaded oil droplet under water on the multilayer coating was continuously depleted from ~158° to 0° (Fig. 4A black curve), and eventually the oil wettability in the

Open Access Article. Published on 10 Mawuwani 2017. Downloaded on 2025-12-08 16:58:14.
This article is licensed under a Creative Commons Attribution-NonCommercial 3.0 Unported Licence.

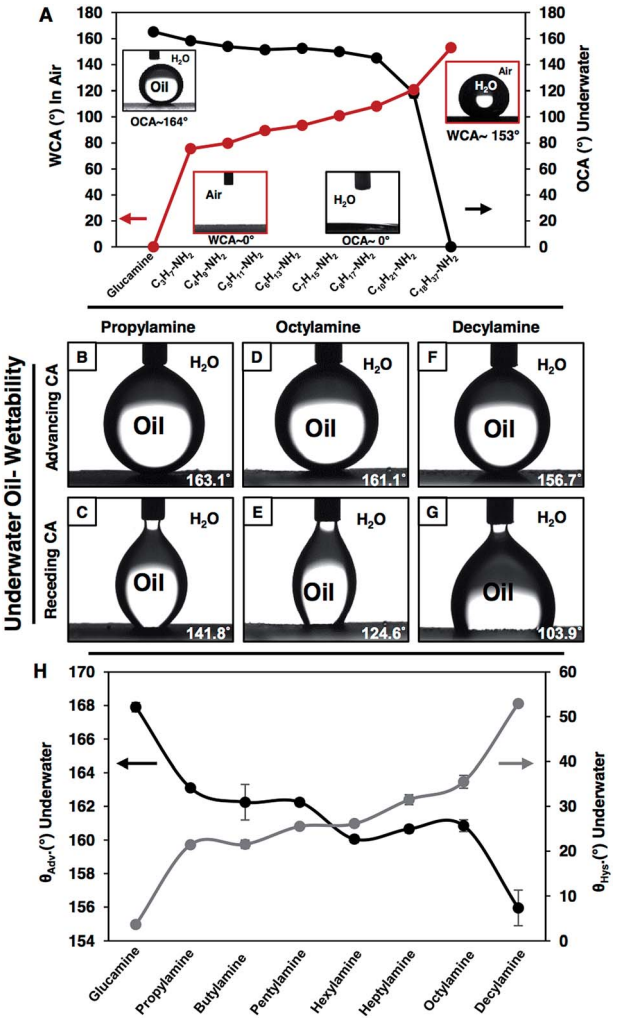

Fig. 4 (A) The plot is illustrating the controlled and extreme change in both the WCA (red line) in air and the OCA (black line) under water through facile post chemical modification with strategically selected primary amine containing small molecules. The post chemical modification of the multilayers with glucamine and ODA molecules provided extremes of oil and water wettability both in air (inset, red boxes) and under water (inset, black boxes). (B–G) Under water advancing (B, D and F) and receding (C, E and G) OCA of the beaded oil droplets on the multilayers of the NCs that were post chemically modified with propylamine (B and C), octylamine (D and E) and decylamine (F and G). (H) The plot shows the change in advancing OCA (black) and contact angle hysteresis (grey) under water after post chemical treatment of the multilayers with selected (hydrophilic, less hydrophobic and more hydrophobic) small molecules.

multilayer coating was transformed from superoleophobic (extreme repellency to oil) to superoleophilic (extreme attraction to oil) as shown in Fig. 4A. Such continuous and extreme regulation of both oil and water wettability using a single polymeric coating through facile and direct covalent bonding (the Michael addition reaction) is yet to be introduced in the literature.

Furthermore, other special oil-wettability under water was discovered in the multilayer coating during this strategic post chemical modification of the multilayers of the NCs with amine containing small molecules—which have various hydrocarbon tails. On all occasions, the oil droplets were beaded on the differently post modified multilayers with advancing OCAs above 155°. However, OCA hysteresis was gradually enhanced from ~21° (propylamine) to 53° (decylamine) with increasing hydrocarbon tail length from $-C_3H_7$ (propylamine; Fig. 4B and C) to $-C_{10}H_{21}$ (decylamine; Fig. 4F and G) in the reacted small molecules as shown in Fig. 4H. This unambiguously revealed the gradual increment in adhesive interaction between the beaded oil droplets and multilayer coatings, even though the beaded droplets were extremely repelled by the coatings with an $\theta_{adv.}$ above 155° (Fig. 4B, D, F and H; black curve), and eventually resulted in more deformation of the beaded oil droplets at the liquid/solid interface during the recession of the oil droplets as shown in Fig. 4C, E and G, and a gradual change in CA hysteresis was observed as noted in Fig. 4H (grey curve). However, post modification of the same multilayers of the NCs with small molecules having a much longer hydrocarbon tail (ODA, $-C_{18}H_{37}$) provided a completely different super-wettability—called underwater superoleophilicity—which soaked oil with a 0° contact angle (as discussed in the previous section, Fig. 4A). Thus, the current approach strategically exploited the 1,4-conjugate addition reaction in tailoring the liquid (water and oil) wettability including extremes of wettability and special wettability (adhesive, but with extreme liquid repellency) on solid surfaces both in air (for water wettability) and under water (for oil wettability) through the controlled modulation of chemical functionality in the reactive multilayers of the NCs.

The topography of the coating is another important criteria that confers the heterogeneous wettability of liquids (oil and water) on solid surfaces both in air and under water. In the past various different approaches—which are generally either complex or require specialized equipment—[59–62] have been introduced to tailor the topography of the materials for adopting adhesive, but extreme, liquid repellent interfaces both in air and under water. The current approach provides a simple avenue to tune the appropriate topography in the multilayers of the NCs for adopting desired special wettability of liquids through facile and controlled regulation on the LbL deposition cycles as mentioned before. The ODA-modified multilayers of the NCs display extreme water repellency with an advancing WCA ~167° after 8 bilayer depositions, and the receding WCA was measured to be ~159° as shown in Fig. 5C and D. However, after 9 bilayer depositions, the same multilayer coating that was constructed from the NC and BPEI was observed to be non-adhesive superhydrophobic with advancing and receding WCAs ~168° and ~165° respectively as shown in Fig. 5E and F. Similarly, the oil-wettability under water was modulated in the glucamine treated multilayers of the NCs by simple control in the LbL deposition cycles. The glucamine treated multilayers of the NCs displayed adhesive superoleophobicity with an advancing OCA ~166° and with a contact angle hysteresis ~34° after 7 bilayer depositions, and the shape of the beaded oil droplets was significantly deformed at the oil/solid interface as shown in Fig. 5G and H. Whereas, after 8 bilayer depositions, the same multilayer of the NCs was found to be non-adhesive with an advancing OCA ~167° (Fig. 5I) and with a contact

This journal is © The Royal Society of Chemistry 2017

Open Access Article. Published on 10 Mawuwani 2017. Downloaded on 2025-12-08 16:58:14.
This article is licensed under a Creative Commons Attribution-NonCommercial 3.0 Unported Licence.

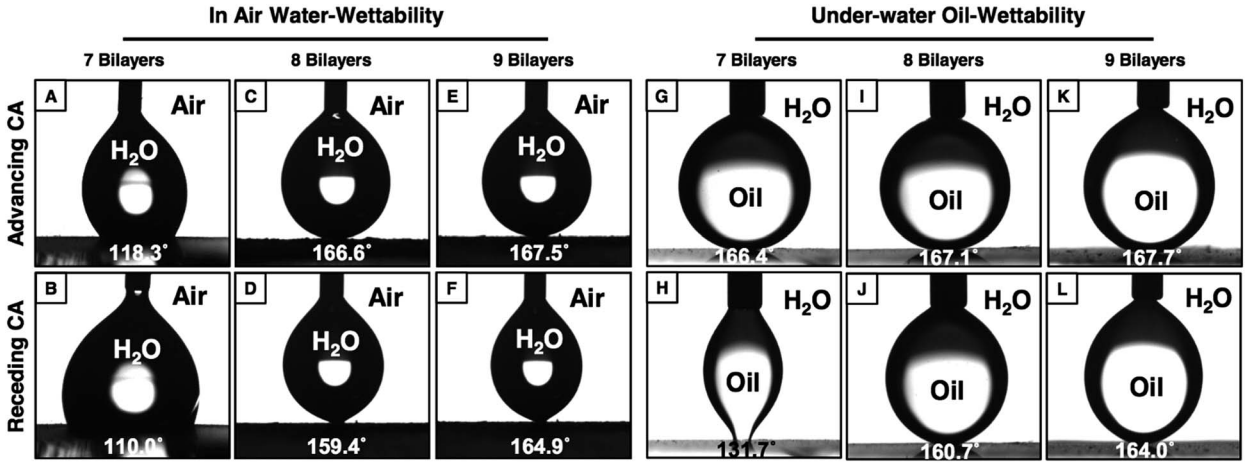

Fig. 5 (A–L) Advancing (A, C, E, G, I and K) and receding (B, D, F, H, J and L) contact angle images of both the beaded water (A–F, in air) and oil (G–L, under water) phases on the multilayers (7 bilayers: A and B, and G and H; 8 bilayers: C and D, and I and J; 9 bilayers: E and F, and K and L) of the NCs that were post chemically modified with ODA (A–F) and glucamine (G–L).

angle hysteresis ~6°, and this multilayer of the NCs became even more non-adhesive superoleophobic with an advancing OCA ~168° and a contact angle hysteresis ~4° after 9 bilayer depositions (Fig. 5K and L). The whole amount of beaded oil completely receded back without a noticeable deformation of the shape of the beaded oil droplets at the oil/solid interfaces as shown in Fig. 5J and L.

Thus, the current design of a 'reactive' multilayer construction through covalent-LbL deposition allowed us to examine independently the role of the essential parameters—(1) topography and (2) chemical functionality—which confer the heterogeneous liquid wettability on a solid surface, without perturbing the other parameters at the same time. For example, the effect of the change in chemical functionality could be studied independently without perturbing the topography of the material, and *vice versa*. The heterogeneous wettability of water and oil in air and under water respectively has often been described by adopting the Cassie–Baxter model,[4] where either the metastable trapped air (for water wettability in air) or the confined liquid water layer (for oil-wettability under water) within the featured surface of the material were attributed to the heterogeneous wettability for both water and oil respectively through limited access to the contact area between the solid surface and respective beaded liquid phases. The fraction of the contact area between the beaded liquid (water and oil) phase and multilayer of the NCs (that were either modified with ODA or glucamine) was estimated using eqn (1) and (2), where θ and θ_r are the liquid (water/oil) contact angles on a multilayer of BPEI/5Acl (smooth surface, 9 bilayers) and multilayer of the NCs in the presence of salt (featured surface; 9 bilayers) respectively.

$$\cos\theta_r = f_1 \cos\theta - f_2 \quad (1)$$

$$f_1 + f_2 = 1 \quad (2)$$

The fraction of the solid contact area and either the trapped air or confined water contact area with the respective beaded liquid (water and oil) phases are labelled as f_1 and f_2, respectively.

The fraction of the solid contact area with the beaded water droplet on the strategically post modified multilayers of the NCs (in the presence of salt) in air was noticed to gradually decrease with the increasing hydrocarbon tail length of the amine containing small molecules from 0.844 ($-C_3H_7$: propylamine) to 0.091 ($-C_{18}H_{37}$: octadecylamine) as shown in Fig. 6J (red curve). As a consequence, the hydrophobicity in the multilayers of the NCs was progressively increased, and eventually, the multilayers of the NCs were embedded with superhydrophobicity (Fig. 6C) after ODA treatment (Fig. 6A). However, on increasing the hydrophobic tail length of the reacted small molecules in the post modified multilayers of the NCs from $-C_3H_7$ (propylamine) to $-C_{10}H_{21}$ (decylamine), the change in the fraction of the solid contact area for the beaded oil phase on the multilayer coatings was comparatively more sluggish under water, and the solid contact area was only increased from 0.067 to 0.276 as shown in Fig. 6J (black curve). This controlled and sluggish change in the fraction of the solid contact area with the beaded oil phase effectively controls the adhesive interaction between the multilayers and beaded oil phase—but the multilayer surfaces continued to display extreme oil repellency with an advancing OCA above 155° as the fraction of the solid contact area with the beaded liquid phase remained low in general, even after post chemical modification with decylamine molecules. However, the fraction of the solid contact area suddenly increased to 1 on the modification of the multilayers with ODA molecules—which essentially transformed the material to be underwater superoleophilic (Fig. 6B). Thus, the same multilayers of the NCs (9 bilayers) with an identical topography but a strategic post chemical modification (Fig. 6A, D and G) with appropriate small molecules essentially controlled the contact area access between the solid surface (multilayers of the NCs) and beaded liquid (water/oil) phases both under water (for oil droplets; Fig. 6B, E and H) and in air (for water droplets; Fig. 6C, F and I), and eventually tailored the liquid wettability both in air and under

Open Access Article. Published on 10 Mawuwani 2017. Downloaded on 2025-12-08 16:58:14.
This article is licensed under a Creative Commons Attribution-NonCommercial 3.0 Unported Licence.

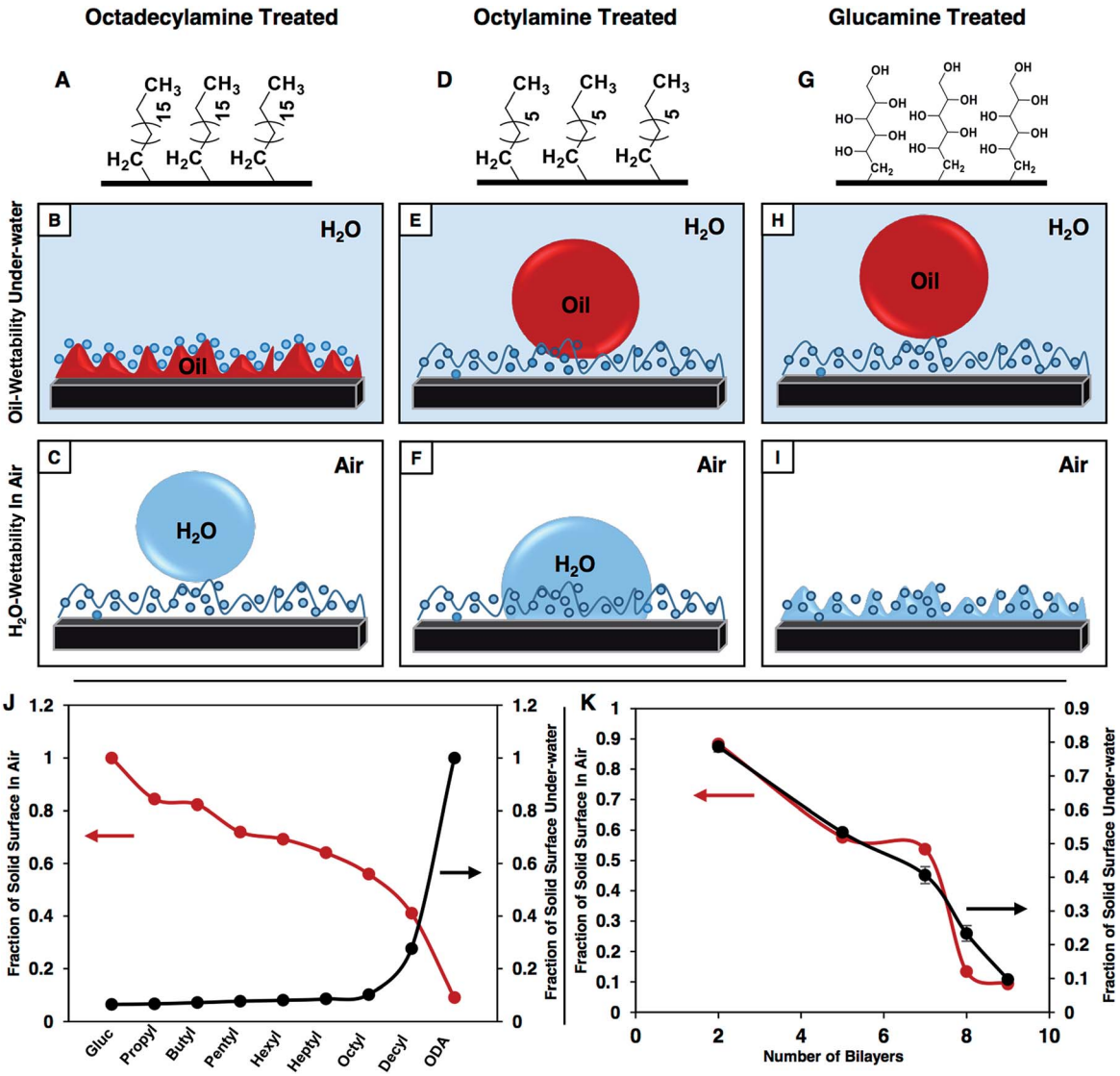

Fig. 6 (A, D and G) Schematic representation of the multilayers (9 bilayers, in the presence of salt) of the NCs that were chemically post-modified with octadecylamine (A), octylamine (D) and glucamine (G). (B–I) Schematic illustrations of the wettability of oil (under water (B, E and H)) and water (in air (C, F and I)) phases on the multilayers that are chemically functionalized with ODA (B and C), octylamine (E and F) and glucamine (H and I) molecules. (J and K) Graphical overview of the change in the fraction of the solid surface area with the beaded water (red line) and oil (black line) phases both in air (red line) and under water (black line) through the modulation of chemical functionality (J) in the multilayers and controlling the deposition cycles (K) during multilayer construction.

water. However, the trends in the change of the fraction of the solid contact area with beaded liquid phases both in air and under water were noted to be considerably different, which again suggested that the stability of the impregnated phases (water and oil)—which are hypothesized to control the homogeneous/heterogeneous wettability of the respective liquids in air and under water—might be different even though the multilayers of the NCs with identical topography were post modified with the same chemically functional molecules. As a consequence, with increasing hydrocarbon tail length from $-C_3H_7$ (propylamine) to $-C_{10}H_{21}$ (decylamine) in the reacted small molecules in the multilayer of the NCs, the hydrophobicity (in air) was increased from ~76° to ~121°. In comparison, the multilayers of the NCs were proficient in displaying superoleophobicity (with an advancing OCA above 155°) under water, and the adhesive property was increased with increasing hydrocarbon tail length in the reacted small molecules (Fig. S5†).

Next, the effect of consecutive LbL deposition (or the topography of multilayers) of the NCs on the fraction of the solid contact area with the respective liquid (either water or oil) phase was examined both in air and under water, where the chemical functionalities (ODA-treatment (Fig. 6A) for water wettability in air and glucamine-treatment (Fig. 6G) for oil wettability under water) of the multilayers were kept unaltered during the entire study. The fraction of the solid contact area of the beaded water droplet on the multilayer of the NCs (which was post modified with ODA molecules) in air was initially decreased slowly from 0.88 (2 bilayers) to 0.54 (7 bilayers) with

This journal is © The Royal Society of Chemistry 2017

Open Access Article. Published on 10 Mawuwani 2017. Downloaded on 2025-12-08 16:58:14.
This article is licensed under a Creative Commons Attribution-NonCommercial 3.0 Unported Licence.

increasing the number of LbL deposition cycles, and after 7 bilayer depositions, the fraction of the solid contact area had significantly dropped as shown in Fig. 6K (red curve), and eventually provided superhydrophobicity to the multilayers. However, in the case of the underwater beaded oil droplet on the multilayer of the NCs, that was post functionalized with glucamine molecules, the fraction of solid contact area was decreased following a 'linear-like' trend from 0.78 to 0.09 on increasing the number of consecutive LbL dipping cycles as observed in Fig. 6K (black curve). Thus, this analysis revealed that both the chemical functionality and topography of the material actively contribute to the heterogeneous wettability of both water and oil in air and under water respectively through the appropriate change in the solid contact area with beaded liquid droplets.

Physical and chemical durability of the anti-fouling properties

In general, several reported anti-fouling materials (having either superhydrophobicity in air or superoleophobicity underwater), which are developed from metal oxides,[38–41] polymeric hydrogels[3,14,18,42–44] or other organic substances,[45–47] are highly delicate and susceptible to perturbation of the chemical functionality and/or the topography that exist in the material, after exposure to common physical manipulations or harsh chemical environments.[27–31,48] So, the synthesized and optically semitransparent multilayers that are embedded with super-anti-fouling properties were exposed to various harsh chemical and physical insults to investigate the durability of the embedded anti-liquid-wettability properties in the strategically post-modified multilayers of the NCs. First, the multilayers of the NCs were placed under a continuous stream of sand (60 g) that was dropped from a 20 cm height, (Fig. S7H and I†) and at the end, the materials were recovered with intact anti-fouling properties. Both the water and the oil droplets were beaded on the materials with advancing CAs $\geq 160^\circ$ and CA hysteresis $\leq 10^\circ$ both in air and under water. A very similar result was also noticed after performing another conventional abrasive test, recognized as the adhesive tape test (Fig. S7A†), where adhesive tape was manually placed on the multilayers of the NCs, and a load applied (50 g) to facilitate the uniform contact between the adhesive surface and multilayer coatings, prior to peeling off the adhesive tape from the multilayers of the NCs (Table 1). Next, the multilayer coatings were exposed to complex and corrosive aqueous solutions including extremes of pH (pH 1 and pH 11), SDS surfactant (model detergent, 1 mM), artificial sea water (having large salt concentration) and river water (having various bio-contaminants). However, the multilayer coatings retained the ability to repel both water (in air) and oil (under water) droplets with advancing CAs $>160^\circ$ and CA hysteresis $<10^\circ$ as listed in Table 1 and Fig. S6.† This impeccable durability of the liquid wettability in the synthesized materials might arise from the covalent crosslinks in the multilayers through the 1,4-conjugate addition reaction.

Multilayer coatings on various substrates

There are few reported approaches[47,63–66] in the literature that can coat various substrates irrespective of the chemical composition (metallic, polymeric, hydrophilic, hydrophobic *etc.*), geometry and physical states (rigid, flexible, smooth, fibrous *etc.*) of the substrates. Here, the current covalent and 'reactive' LbL-deposition approach allows the coating of various substrates including smooth (glass or Al-foil), fibrous (synthetic fabric) and underwater oleophobic/hydrophobic (wood surface) substrates with multilayers of the NCs to decorate the substrates with the desired anti-wettability properties in air and under water through facile and appropriate post chemical modification. The uncoated synthetic fabric, which soaked both water and oil in air and under water respectively with a CA of 0° (Fig. 7A and J), was observed to display extreme liquid (water/oil) repellency both in air and under water with an advancing contact angle above 160° (Fig. 7D and M), and the respective liquid droplets (red color aids visual inspection) were beaded on the appropriately post functionalized multilayer coatings with spherical shapes (Fig. 7G and P), which further revealed the existence of both superhydrophobicity (in air) and superoleophobicity (under water) in the multilayer coatings. Similarly, a smooth metal surface, Al-foil, which is inherently oleophobic (OCA $\sim 138^\circ$; under water; Fig. 7B) and hydrophilic (WCA $\sim 64^\circ$ in air; Fig. 7K), was decorated with under water superoleophobicity (an advancing OCA $\sim 165^\circ$, Fig. 7E and H) and superhydrophobicity (an advancing OCA $\sim 168^\circ$; Fig. 7N and Q) in air by exploiting the current design. Another model substrate—wood—which moderately repels both oil (CA $\sim 136^\circ$ under water; Fig. 7C) and water (CA $\sim 114^\circ$ in air; Fig. 7L) became superoleophobic under water and superhydrophobic in air after coating the substrate with multilayers of the NCs that were post-chemically modified with appropriate small molecules through the facile Michael addition reaction. The stability of the coating on these different substrates was investigated by the adhesive tape peeling test, and the polymeric coating was found to have uninterrupted anti-fouling properties even after the adhesive tape peeling test. Thus, the current strategy could be highly useful for marine and other relevant applications including prevention of oil contamination, oil/water separation, protein crystallization, developing smart fabrics *etc.*. Moreover, this approach would enable the coating of a wide range of other

Table 1 Both the advancing liquid (oil/water) contact angle and respective contact angle hysteresis in air and under water after exposing the multilayers to different physical conditions (sand drop test and adhesive tape test) and chemical (extremes of pH (pH 1, 11), river water, sea water and surfactant (SDS 1 mM)) contaminated aqueous environments

Physical and chemical insults	Underwater superoleophobicity		In air superhydrophobicity	
	$\theta_{adv.}$ (°)	$\theta_{hys.}$ (°)	$\theta_{adv.}$ (°)	$\theta_{hys.}$ (°)
Adhesive tape	165.9 ± 1.7	5.8 ± 2.4	160.5 ± 1.1	9.3 ± 1.6
Sand drop	165.2 ± 0.2	5.1 ± 0.7	164.8 ± 1.9	9.7 ± 1.4
Acid water	165.7 ± 0.7	5.3 ± 0.8	164.4 ± 0.4	4.1 ± 0.6
River water	166.6 ± 0.3	8.1 ± 0.5	161.0 ± 0.3	2.1 ± 1.3
Alkaline water	165.9 ± 0.7	6.1 ± 2.2	164.9 ± 1.5	5.3 ± 2.1
SDS water	165.7 ± 0.5	3.0 ± 1.1	165.7 ± 0.6	1.8 ± 1.4
Sea water	166.3 ± 1.0	2.5 ± 1.4	166.9 ± 0.8	6.0 ± 0.8

Open Access Article. Published on 10 Mawuwani 2017. Downloaded on 2025-12-08 16:58:14.
This article is licensed under a Creative Commons Attribution-NonCommercial 3.0 Unported Licence.

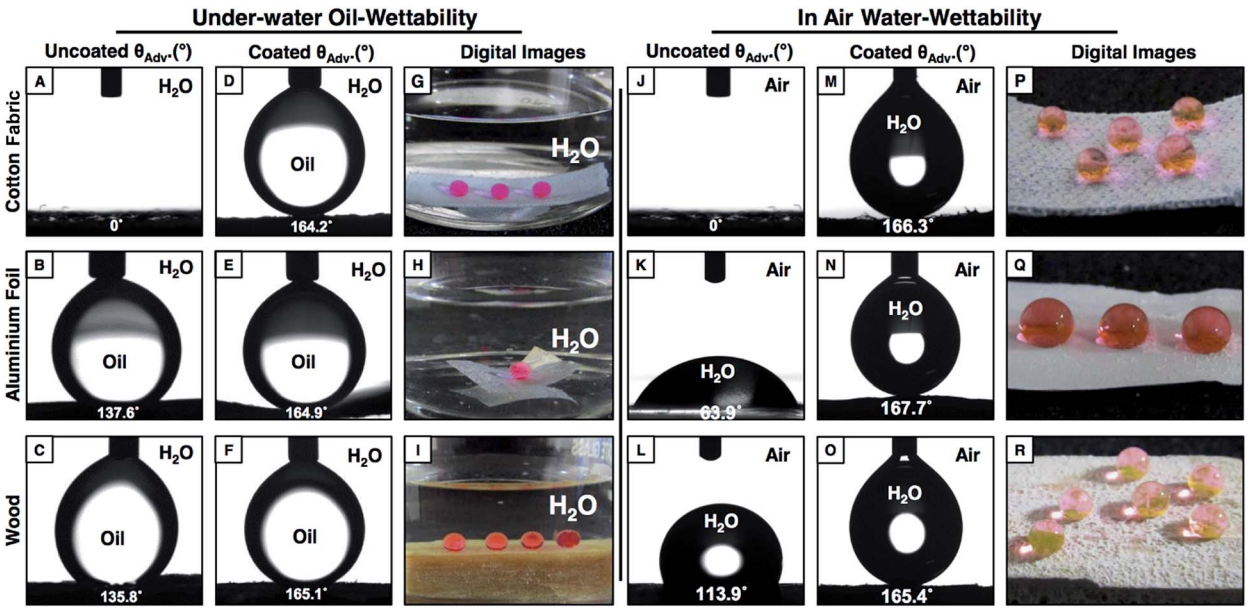

Fig. 7 (A–I) Contact angle images (A–F) and digital images (G–I) of the beaded oil droplets (red color aids visual inspection) on both the uncoated (A–C) and multilayer (9 bilayers, treated with glucamine) coated (D–I) flexible ((A, D and G) fibrous cotton substrate and (B, E and H) Al-foil) and rigid ((C, F and I) wood) substrates under water. (J–R) Contact angle images (J–O) and digital images (P–R) showing the change in water wettability (in air) before (J–L) and after (M–R) decorating the cotton fabric (J, M and P), Al-foil (K, N and Q) and wood (L, O and R) with multilayers of the NCs (9 bilayers, post treated with ODA).

useful substrates with desired anti-fouling properties for a specific or wide variety of applications related to energy, health and the environment.

Conclusions

Here, we have developed a multilayer construction by strategically exploiting a simple covalent-LbL deposition technique in combination with a robust 1,4-conjugate addition reaction between acrylate and amine groups for the controlled and extreme regulation of water and oil wettability both in air and under water respectively. The growth of multilayers of the NCs (that formed when mixing BPEI and 5Acl in methanol) was comparatively rapid and exponential in the presence of salt, and provided appropriate topography to display extreme liquid wettability properties including superhydrophobicity/superhydrophilicity in air and superoleophobicity/superoleophilicity under water. Moreover, consecutive LbL deposition allowed facile control over the topography of the multilayer coatings, to adopt special adhesive anti-fouling properties through control of the fraction of the contact area of the solid with the beaded oil droplets. On the other hand, residual acrylate groups in the multilayers provided a convenient basis for the precise control of the fraction of the solid contact area with the beaded liquid phases both under water and in air through suitable and appropriate post chemical modification of the multilayers of the NCs with small molecules *via* the 1,4-conjugate addition reaction, and the appropriately post-functionalized multilayers of the NCs were eventually embedded with various special water (in air) and oil (under water) wettability properties. The current design allowed a comprehensive and comparative investigation on the homogeneous/heterogeneous wettability of both water and oil in air and under water respectively using a single material—that is the 'reactive' and covalent multilayer coatings of the NCs. The extreme and special wettability of both the water (in air) and the oil phases (under water) was successfully adopted by tailoring the fraction of the solid contact area with the beaded liquid droplets through both the change in chemical functionality and topography of the material. However, the same extent of change in the chemistry and topography in the material has an independent implication on the water (in air) and oil (under water) wettability. Moreover, the synthesized multilayers of the NCs were able to sustain various physical and chemical insults without compromising the anti-fouling property of the materials, and the current strategy also provided a facile avenue to decorate a wide variety of substrates with the desired anti-fouling properties. Thus, this material has the ability to be general and would be useful in various relevant applications including the synthesis of patterned interfaces through site-specific functionalization of the 'reactive' multilayers of the NCs, and could be useful in various advanced applications.[67]

Acknowledgements

We would like to thank the Science and Engineering Research Board (YSS/2015/000818), Department of Science and Technology and the Board of Research in Nuclear Sciences (BRNS) (34/20/31/2016-BRNS, DAE-YSRA), Department of Atomic Energy (DAE) for financial support. We acknowledge the generous help from CIF and the Department of Chemistry, Indian Institute of Technology-Guwahati. We are thankful to Dr

Open Access Article. Published on 10 Mawuwani 2017. Downloaded on 2025-12-08 16:58:14.
This article is licensed under a Creative Commons Attribution-NonCommercial 3.0 Unported Licence.

Devasish Chowdhury and the Institute of Advanced Study in Science and Technology (IASST) for their kind and continuous support in performing the FESEM characterization of some samples. Ms Dibyangana Parbat and Mr Adil Majeed Rather are grateful to IIT-Guwahati for their Institute PhD fellowships.

References

1 L. Feng, S. H. Li, Y. S. Li, H. J. Li, L. J. Zhang, J. Zhai, Y. L. Song, B. Q. Liu, L. Jiang and D. B. Zhu, *Adv. Mater.*, 2002, **14**, 1857.
2 X. M. Li, D. Reinhoudt and M. Crego-Calama, *Chem. Soc. Rev.*, 2007, **36**, 1350.
3 M. J. Liu, S. T. Wang, Z. X. Wei, Y. L. Song and L. Jiang, *Adv. Mater.*, 2009, **21**, 665.
4 Z. Chu, Y. Feng and S. Seeger, *Angew. Chem., Int. Ed.*, 2015, **54**, 2328.
5 B. Su, Y. Tian and L. Jiang, *J. Am. Chem. Soc.*, 2016, **138**, 1727.
6 X. Yao, J. Gao, Y. Song and L. Jiang, *Adv. Funct. Mater.*, 2011, **21**, 4270.
7 A. K. Kota, G. Kwon, W. Choi, J. M. Mabry and A. Tuteja, *Nat. Commun.*, 2012, **3**, 1.
8 E. Ueda and P. A. Levkin, *Adv. Mater.*, 2013, **25**, 1234.
9 Y. Wu, B. Su, L. Jiang and A. J. Heeger, *Adv. Mater.*, 2013, **25**, 6526.
10 Z. Shi, W. Zhang, F. Zhang, X. Liu, D. Wang, J. Jin and L. Jiang, *Adv. Mater.*, 2013, **25**, 2422.
11 M. Tao, L. Xue, F. Liu and L. Jiang, *Adv. Mater.*, 2014, **26**, 2943.
12 L. Wen, Y. Tian and L. Jiang, *Angew. Chem., Int. Ed.*, 2015, **54**, 3387.
13 Z. Chu, Y. Feng and S. Seeger, *Angew. Chem., Int. Ed.*, 2015, **54**, 2328.
14 Y. Cai, Q. Lu, X. Guo, S. Wang, J. Qiao and L. Jiang, *Adv. Mater.*, 2015, **27**, 4162.
15 A. Gao, Q. Wu, D. Wang, Y. Ha, Z. Chen and P. Yang, *Adv. Mater.*, 2016, **28**, 579.
16 C. Li, M. Boban, S. A. Snyder, S. P. R. Kobaku, G. Kwon, G. Mehta and A. Tuteja, *Adv. Funct. Mater.*, 2016, **26**, 6121.
17 C. Yu, M. Z. Dong, J. Wang, K. Li and L. Jiang, *Adv. Funct. Mater.*, 2016, **26**, 3236.
18 K. Chen, S. Zhou and L. Wu, *ACS Nano*, 2016, **10**, 1386.
19 M. Wu, B. Ma, T. Pan, S. Chen and J. Sun, *Adv. Funct. Mater.*, 2016, **26**, 569.
20 S. T. Yohe, J. D. Freedman, E. J. Falde, Y. L. Colson and M. W. Grinstaff, *Adv. Funct. Mater.*, 2013, **23**, 3628.
21 A. B. D. Cassie and S. Baxter, *Trans. Faraday Soc.*, 1944, **40**, 546.
22 A. B. D. Cassie and S. Baxter, *Nature*, 1945, **155**, 21.
23 A. Tuteja, W. Choi, M. Ma, J. M. Mabry, S. A. Mazzella, G. C. Rutledge, G. H. Mckinley and R. E. Cohen, *Science*, 2007, **318**, 1618.
24 X. M. Li, D. Reinhoudt and M. Crego-Calama, *Chem. Soc. Rev.*, 2007, **36**, 1350.
25 X. Feng and L. Jiang, *Adv. Mater.*, 2006, **18**, 3063.
26 Y. Y. Yan, N. Gao and W. Barthlott, *Adv. Colloid Interface Sci.*, 2011, **169**, 80.
27 G. R. J. Artus, S. Jung, J. Zimmermann, H. P. Gautschi, K. Marquardt and S. Seeger, *Adv. Mater.*, 2006, **18**, 2758.
28 Y. H. Xiu, Y. Liu, D. W. Hess and C. P. Wong, *Nanotechnology*, 2010, **21**(15), 155705.
29 T. Verho, C. Bower, P. Andrew, S. Franssila, O. Ikkala and R. H. A. Ras, *Adv. Mater.*, 2011, **23**, 673.
30 L. Ionov and A. Synytska, *Phys. Chem. Chem. Phys.*, 2012, **14**, 10497.
31 U. Manna and D. M. Lynn, *Adv. Mater.*, 2013, **25**, 5104.
32 X. Deng, L. Mammen, Y. Zhao, P. Lellig, K. Mullen, C. Li, H. J. Butt and D. Vollmer, *Adv. Mater.*, 2011, **23**, 2962.
33 X. Deng, L. Mammen, H. J. Butt and D. Vollmer, *Science*, 2012, **335**, 67.
34 U. Manna, M. C. D. Carter and D. M. Lynn, *Adv. Mater.*, 2013, **25**, 3085.
35 J. E. Mates, I. S. Bayer, J. M. Palumbo, P. J. Carroll and C. M. Megaridis, *Nat. Commun.*, 2015, **6**, 8874.
36 M. Paven, R. Fuchs, T. Yakabe, D. Vollmer, M. Kappl, A. N. Itakura and H. J. Butt, *Adv. Funct. Mater.*, 2016, **26**, 4914.
37 X. Tian, T. Verho and R. H. A. Ras, *Science*, 2016, **352**, 142.
38 X. Liu, J. Zhou, Z. Xue, J. Gao, J. Meng, S. Wang and L. Jiang, *Adv. Mater.*, 2012, **24**, 3401.
39 F. Zhang, W. B. Zhang, Z. Shi, D. Wang, J. Jian and L. Jiang, *Adv. Mater.*, 2013, **25**, 4192.
40 Z. Cheng, H. Lai, Y. Du, K. Fu, R. Hou, C. Li, N. Zhang and K. Sun, *ACS Appl. Mater. Interfaces*, 2014, **6**, 636.
41 J. Yong, F. Chen, Q. Yang, U. Farooq and X. Hou, *J. Mater. Chem. A*, 2015, **3**, 10703.
42 L. Lin, M. J. Liu, L. Chen, P. P. Chen, J. Ma, D. Han and L. Jiang, *Adv. Mater.*, 2010, **22**, 4826.
43 Z. Xue, S. Wang, L. Lin, L. Chen, M. Liu, L. Feng and L. Jiang, *Adv. Mater.*, 2011, **23**, 4270.
44 S. Gao, J. Sun, P. Liu, F. Zhang, W. Zhang, S. Yuan, J. Li and J. Jin, *Adv. Mater.*, 2016, **28**, 5307.
45 L. P. Xu, J. Zhao, B. Su, X. Liu, J. Peng, Y. Liu, H. Liu, G. Yang, L. Jiang, Y. Wen, X. Zhang and S. Wang, *Adv. Mater.*, 2013, **28**, 606.
46 L. P. J. Xu, T. Peng, Y. B. Liu, Y. Q. Wen, X. J. Zhang, L. Jiang and S. T. Wang, *ACS Nano*, 2013, **7**, 5077.
47 W. Ma, H. Xu and A. Takahara, *Adv. Mater. Interfaces*, 2014, **1**, 1300092.
48 T. Guo, L. Heng, M. Wang, J. Wang and L. Jiang, Robust, *Adv. Mater.*, 2016, **28**, 8505.
49 R. A. Farrer, C. N. LaFratta, L. Li, J. Praino, M. J. Naughton, B. E. A. Saleh, M. C. Teich and J. T. Fourkas, *J. Am. Chem. Soc.*, 2006, **128**, 1796.
50 G. Wang, Y. Fang, P. Kim, A. Hayek, M. R. Weatherspoon, J. W. Perry, K. H. Sandhage, S. R. Marder and S. C. Jones, *Adv. Funct. Mater.*, 2009, **19**, 2768.
51 J. Ford, S. R. Marder and S. Yang, *Chem. Mater.*, 2009, **21**, 476.
52 S. L. Bechler and D. M. Lynn, *Biomacromolecules*, 2012, **13**, 1523.
53 A. M. Rather and U. Manna, *Chem. Mater.*, 2016, **28**, 8689.
54 H. Zhu, Z. Guo and W. Liu, *Chem. Commun.*, 2014, **50**, 3900.

Open Access Article. Published on 10 Mawuwani 2017. Downloaded on 2025-12-08 16:58:14.
This article is licensed under a Creative Commons Attribution-NonCommercial 3.0 Unported Licence.

55 C. Tan, P. Cai, L. Xu, N. Yang, Z. Xi and Q. Li, *Appl. Surf. Sci.*, 2015, **349**, 516.
56 Z. Cheng, H. Lai, Y. Du, K. Fu, R. Hou, N. Zhang and K. Sun, *ACS Appl. Mater. Interfaces*, 2013, **5**, 11363.
57 Z. Cheng, H. Liu, H. Lai, Y. Du, K. Fu, C. Li, J. Yu, N. Zhang and K. Sun, *ACS Appl. Mater. Interfaces*, 2015, **7**, 20410.
58 M. J. Nine, T. T. Tung, F. Alotaibi, D. N. H. Tran and D. Losic, *ACS Appl. Mater. Interfaces*, 2017, **9**, 8393.
59 X. Yang, X. Liu, Y. Lu, S. Zhou, M. Gao, J. Song and W. Xu, *Sci. Rep.*, 2016, **6**, 23985.
60 D. Wu, S. Z. Wu, Q. D. Chen, Y. L. Zhang, J. Yao, X. Yao, L. G. Niu, J. N. Wang and L. Jiang, *Adv. Mater.*, 2011, **23**, 545.
61 X. Yao, J. Gao, Y. Song and L. Jiang, *Adv. Funct. Mater.*, 2011, **21**, 4270.
62 Y. Huang, M. Liu, J. Wang, J. Zhou, L. Wang, Y. Song and L. Jiang, *Adv. Funct. Mater.*, 2011, **21**, 4436.
63 S. M. Kang, I. You, W. K. Cho, H. K. Shon, T. G. Lee, I. S. Choi, J. M. Karp and H. Lee, *Angew. Chem., Int. Ed.*, 2010, **49**, 9401.
64 S. T. Yohe and M. W. Grinstaff, *Chem. Commun.*, 2013, **49**, 804.
65 H.-Y. Chen, M. Hirtz, X. Deng, T. Laue, H. Fuchs and J. Lahann, *J. Am. Chem. Soc.*, 2010, **132**, 18023.
66 L. P. Xu, D. Han, X. Wu, Q. Zhang, X. Zhang and S. Wang, *Sci. Rep.*, 2016, **3**, 38016.
67 J. Li, L. Li, X. Du, W. Feng, A. Welle, O. Trapp, M. Grunze, M. Hirtz and P. A. Levkin, *Nano Lett.*, 2015, **15**, 675.

This journal is © The Royal Society of Chemistry 2017